Available online at www.sciencedirect.com
ScienceDirect
Trans. Nonferrous Met. Soc. China 28(2018) 890−895
Transactions of Nonferrous Metals Society of China
www.tnmsc.cn

Effects of secondary phases on texture and mechanical properties of as-extruded Mg−Zn−Er alloys

Ke LIU[1], Jin-xue LIU[1], Shu-bo LI[1], Zhao-hui WANG[1], Wen-bo DU[1], Qing-feng WANG[2]

1. College of Materials Science and Engineering, Beijing University of Technology, Beijing 100124, China;
2. Huadian Electric Power Research Institute, Beijing 100124, China

Received 22 November 2016; accepted 6 July 2017

Abstract: The effects of kinds of secondary phases on texture and mechanical properties of Mg−Zn−Er alloys were investigated. The results suggest that the *I*-phase has a great effect on modification of the texture via the discontinuous dynamic recrystallization mechanism (DDRX), which tends to form well-developed equiaxed recrystallized grains. Meanwhile, the *W*-phase plays an important role in refining the grain size via continuous dynamic recrystallization (CDRX), companied with a higher maximum texture intensity. Thus, the Mg−6Zn−1Er alloy containing *I*-phase shows a performance of higher elongation of 20.4%. The Mg−2Zn−2Er alloy including *W*-phase displays a better tensile strength, and the yield strength (YS) is about 247 MPa.

Key words: Mg−Zn−Er alloy; dynamic recrystallization; texture; tensile properties

1 Introduction

Mg−Zn−RE(−Zr) system alloys attract significant interest because they have both high strength at both room and elevated temperatures [1]. In Mg−Zn−RE(−Zr) alloys, the main ternary phases are the *I*-phase (Mg_3Zn_6RE, icosahedra quasicrystal structure, quasi-periodically ordered) and the *W*-phase ($Mg_3Zn_3RE_2$, cubic structure) [2]. As a secondary phase, the *I*-phase is stable and against the microstructure coarsening at elevated temperature due to the low interfacial energy. Additionally, it plays an important role in enhancing mechanical properties of wrought magnesium alloys [3]. Therefore, the *I*-phase attracts more attentions in Mg−Zn−RE(−Zr) alloy systems. LI et al [4] have reported that the as-cast Mg−Zn−Er alloy strengthened by the *I*-phase exhibited a high tensile strength and good creep-resistant property. YUAN et al [5] have introduced the hot extrusion (HE) process to prepare Mg−Zn−Y alloys and Mg−Zn−Gd alloys strengthened by the *I*-phase, and these alloys exhibited excellent mechanical properties.

However, the appearance of the *I*-phase is generally companied with the presence of the *W*-phase. It was reported that the *W*-phase had weak bonding with the Mg matrix [6]. Besides, the *W*-phase was easily cracked during tensile test in as-cast Mg−Zn−Y−Zr alloys [7]. The diffusive distribution of the *W*-phase in Mg matrix after thermo-mechanical working process pinned the dislocations and contributed some dispersion-strengthening effect to Mg−Zn−RE alloys [8]. YANG et al [9] reported that the uniform distribution of the *W*-phase with a size of less than 1 μm reduced the possibility of cavitation at particles, thereby enhancing the superplastic elongation. On the whole, more attention has been paid to the effect of both the *W*-phase and the *I*-phase on advancing mechanical properties of Mg−Zn−RE alloys. XU et al [10] investigated the mechanical properties of as-extruded Mg−Zn−Y−Zr alloys with different Y contents. The results showed that the strengthening effect of the *I*-phase was better than that of the *W*-phase because of the weak atomic bonding between the *W*-phase and the Mg matrix. However, they did not consider the effect of the volume fraction of the secondary phase on mechanical properties of as-extruded alloys.

Therefore, the Mg−6Zn−1Er and Mg−2Zn−2Er alloys (identified as Alloy A and Alloy B, respectively) which had mostly the same volume fraction of the

Foundation item: Project (51401005) supported by the National Natural Science Foundation of China; Projects (2172013, 2164055) supported by Beijing Natural Science Foundation, China; Project (2016YFB0301101-1) supported by the National Key Research and Development Program, China; Project (2015-RX-L11) supported by TiXin Talents Plan of Beijing University of Technology, China
Corresponding author: Wen-bo DU; Tel/Fax: +86-10-67392917; E-mail: duwb@bjut.edu.cn
DOI: 10.1016/S1003-6326(18)64722-3

secondary phases were prepared in the present work. In Alloy A, the secondary phase was the *I*-phase, and the volume fraction of the *I*-phase was about 3.4%. The secondary phase in Alloy B was the *W*-phase with the volume fraction of 3.2%. The texture and mechanical properties of the as-extruded alloys were investigated. The difference in strengthening effect between the *I*-phase and the *W*-phase with almost the same volume fraction was discussed in order to find the effect of the types of secondary phase on mechanical properties, which would be beneficial to produce a new kind of high-performance magnesium alloy.

2 Experimental

The as-cast alloys were prepared from the pure Mg (99.99%), pure Zn (99.9%) and Mg−30%Er (mass fraction) master alloys in an electric resistance furnace under an anti-oxidizing flux. The melt of about 1200 g was poured into a steel mold, and an ingot with a size of 33 mm × 120 mm × 200 mm was obtained. The as-cast samples were annealed at 400 °C for 10 h, and cooled down in water of 70 °C. The cylinder with a size of 35 mm in diameter and 35 mm in height was obtained by linear cutting from ingot as the original extrusion billet. The billets were hot extruded into rods with a ratio of 10:1 at 400 °C and an extrusion speed of 3 mm/s.

The chemical compositions of as-cast alloys were analyzed with X-ray fluorescence (XRF) analyzer, as given in Table 1. The phase analysis was performed with X-ray diffractometry (XRD) with the Cu K_α radiation. The microstructure observations were carried out with optical microscope (OM, Zeiss-Imager.A2m), scanning electron microscope (SEM, HITACHI S−450) and transmission electron microscope (TEM, JEM−2000FX, JEOL). The texture analyses by using EBSD were conducted with scanning electron microscope (TFE-SEM, JEOL JSM−6500F) operating at 30 kV equipped with TSL-OIM Analysis 5 software. The average grain sizes of as-extruded alloys were measured via a linear intercept method. The samples for OM and SEM observation were mechanically polished and then etched in a solution of 4 mL nitric acid and 96 mL ethanol. Specimens for TEM observation were prepared by ion beam milling at an angle of incidence less than 10°. Samples for texture analysis were prepared by electropolishing with a solution of 60% methanol, 30% glycerol and 10% nitric acid at 25 °C for 10−30 s with a LectroPol-5 electrolytic polisher.

Tensile test was carried out with a DNS−20 universal testing machine under a constant speed of 1.0 mm/min at room temperature. Specimens for the tensile test were made into dog-bone with a size of 5 mm in gauge diameter and 25 mm in gauge length. Three specimens were tested for each sample. All the tensile samples were sectioned in parallel to the extrusion direction for the as-extruded alloys.

Table 1 Chemical compositions of Mg−Zn−Er alloys (mass fraction, %)

Alloy	Zn	Er	Mg	w(Zn)/w(Er)
A	5.9	1.0	Bal.	5.9
B	2.0	2.3	Bal.	0.87

3 Experimental results

3.1 Microstructure of as-cast alloys

The XRD patterns of as-cast alloys are shown in Fig. 1. As suggested by the patterns, Alloy A contains only one kind of secondary phase, i.e. the *I*-phase, while Alloy B only includes the *W*-phase. No other phase is detected within the sensitivity limits of X-ray diffraction (XRD). Figure 2 shows the OM images of the as-

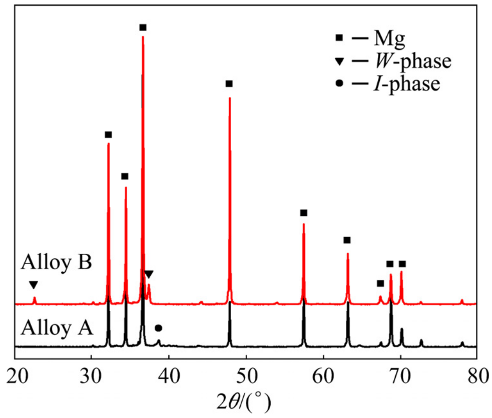

Fig. 1 XRD patterns of as-cast alloys

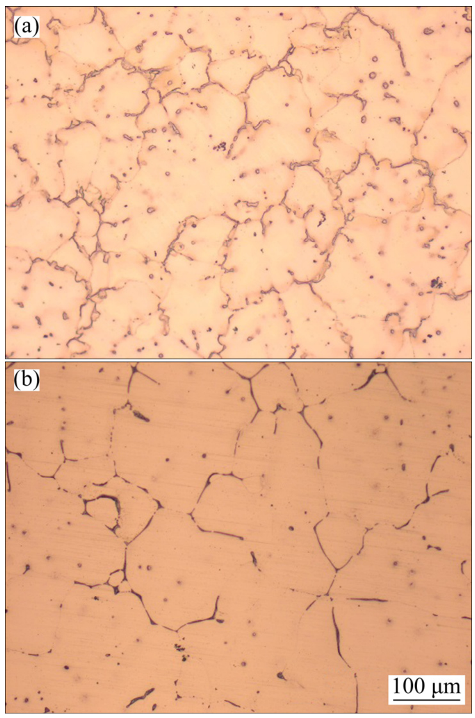

Fig. 2 OM images of as-annealed alloys at 400 °C for 10 h: (a) Alloy A; (b) Alloy B

annealed alloys. It is indicated that both of them are composed of the interdendritic microstructure. The particle-like and strip-like secondary phases are found at matrix and interdendritic boundaries. The volume fractions of the secondary phases in as-cast alloys A and B have been measured by using an image analysis method, the values of which are ~3.4% and ~3.2%, respectively.

3.2 Microstructure of as-extruded alloys

Figure 3 shows the OM and SEM images of the as-extruded alloys along the extrusion direction (ED). It is clearly suggested that the dynamic recrystallization (DRX) took place in the two kinds of alloys during HE. The black regions in Fig. 3(a) and white regions in Fig. 3(b) are the *I*-phase, respectively, while the similar regions in Figs. 3(c) and (d) are the *W*-phase. Alloy A shows a complete DRX microstructure covered by almost equiaxed grains, as shown in Figs. 3(a) and (b). Meanwhile, Alloy B shows a bimodal grain structure consisting of fine grains and unDRXed regions, as shown in Fig. 3(c). The average grain sizes of as-extruded alloys A and B are 9.7 and 5.0 μm, respectively. It is found that the average grain size of the as-extruded Alloy A is almost twice as large as that of the Alloy B.

Figure 4 shows the inverse pole figure (IPF) maps of the as-extruded alloys A and B taken parallel to the extrusion direction (ED) obtained by using EBSD. In the maps, the red color stands for the (0002) basal plane, and the blue color represents the plane lying 90° away from (0002) plane. The nearly identical color of two grains means that the misorientation between grains is small. On the whole, the two as-extruded alloys are mainly composed of the grains exhibiting their (0002) basal plane. Moreover, the orientation of DRX grains is more dispersed in the as-extruded alloy A containing the *I*-phase. Figure 5 displays the pole figures (PF) of as-extruded alloys A and B corresponding to Fig. 4. It is indicated that the two alloys exhibit a fiber texture with the (0002) planes parallel to the extrusion direction, which is found in the as-extruded Mg−Zn−Y−Zr alloys universally. The maximum intensity values of the texture in the as-extruded alloys A and B are ~7.8 and ~13.1, respectively. The maximum intensity value of the texture of the as-extruded Alloy B is 78% higher than that of the as-extruded Alloy A.

3.3 Mechanical properties

The stress−strain curves and the tensile properties of as-extruded alloys at room temperature are shown in Fig. 6. The values of mechanical properties are given in Table 2. It can be found that the values of the ultimate tensile strength (UTS) of as-extruded alloys A and B are almost similar. However, there is a great difference in the yield strength (YS) and the elongation between the Alloy A and the Alloy B. The value of YS of the as-extruded alloy A is about 181 MPa with an elongation of 20.4%. Meanwhile, the YS of the as-extruded alloy B is about 247 MPa with an elongation of 12.1%. It is found that the YS of the as-extruded alloy B is higher than that of the as-extruded alloy A because of the presence of the *W*-phase. The YS of as-extruded alloy B is improved by ~66 MPa, compared with the as-extruded alloy A. Meanwhile, the elongation of as-extruded alloy A is higher than that of the as-extruded alloy B obviously.

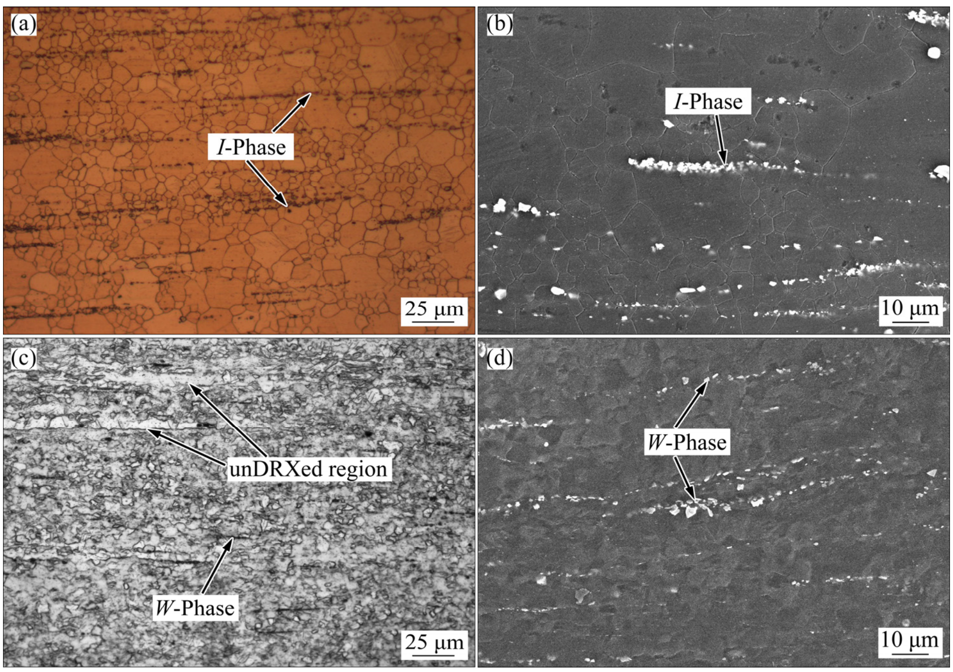

Fig. 3 OM (a, c) and SEM (b, d) images of as-extruded alloys: (a, b) Alloy A; (c, d) Alloy B

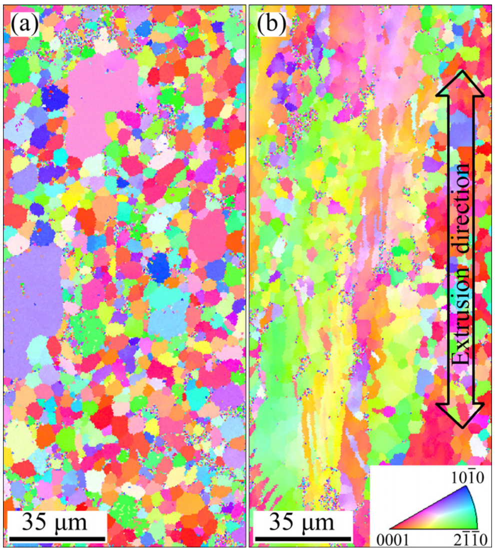

Fig. 4 Inverse pole figure maps of as-extruded alloys: (a) Alloy A; (b) Alloy B

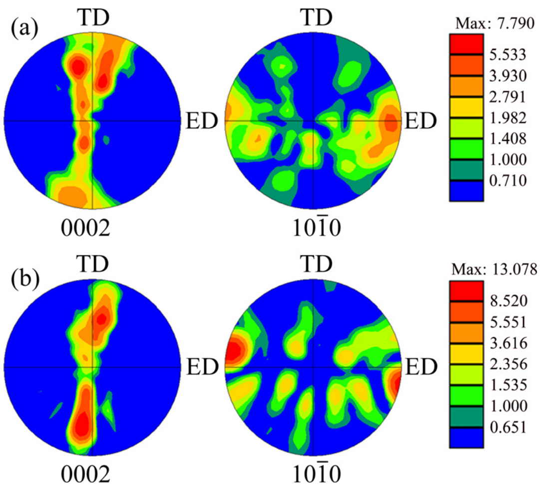

Fig. 5 Pole figures of as-extruded alloys: (a) Alloy A; (b) Alloy B

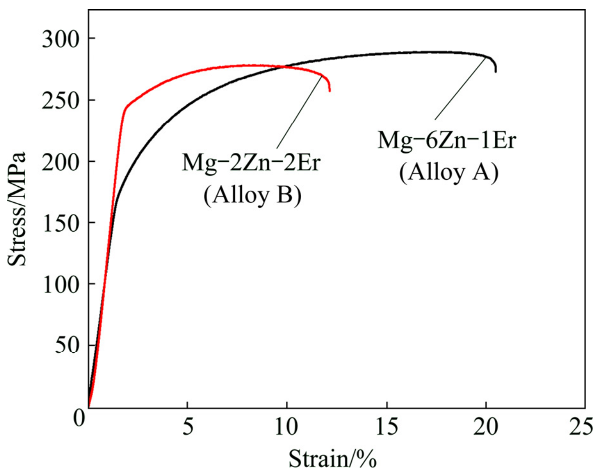

Fig. 6 Stress−strain curves of as-extruded alloys tested under constant speed of 1.0 mm/min at room temperature

Table 2 Mechanical properties of as-extruded Mg−Zn−Er alloys at room temperature

Alloy	Volume fraction of secondary phase/%	UTS/ MPa	YS/ MPa	Elongation/ %
Mg−6Zn−1.0Er	3.4	284	181	20.4
Mg−2Zn−2Er	3.2	279	247	12.1

4 Discussion

It is well known that the magnesium and its alloys are short of ductility because of the hexagonal close-packed (HCP) crystal structure [11]. Thus, the magnesium alloys are usually wrought at high temperature as result of the activation of the DRX. The DRX played an important role in refinement of grains and modification of the texture which strongly influences mechanical properties of magnesium alloys [12−16]. The DRX is considered to be introduced by shear band induced nucleation [17,18], deformation twins induced nucleation [19] and particle stimulated nucleation (PSN) [20,21]. Especially, the PSN has a great effect on developing the high-ductility magnesium alloys. The secondary phase particles have been thought as the heterogeneous nucleation sites for the recrystallized grains with random orientations, leading to a weak texture. It is well known that the addition of Er into Mg−Zn alloys leads to the precipitation of the Mg−Zn−Er ternary phases which mainly includes the *I*-phase (Mg_3Zn_6Er) and the *W*-phase ($Mg_3Zn_3Er_2$) [22]. The presence of the *I*-phase and *W*-phase plays an important role in activating the DRX via PSN.

As reported, the distribution, volume fraction and native physical properties of the secondary phase influence the microstructure of Mg−Zn−Er alloys via DRX [23]. The *I*-phase displays a low interfacial energy, leading to a good bonding with the matrix, and the fivefold and twofold planes of the *I*-phase match with the basal and prismatic planes of the matrix, respectively [24,25]. It generally distributes at the grain boundaries discontinuously as well as at matrix with a round morphology. Meanwhile, the *W*-phase with a face-centered cubic (FCC) structure is coarse and brittle, and thus it is easy to be broken under stress concentration because of impediment of the load transferring from the secondary phase to the matrix [10]. In addition, the *W*-phase was distributed in net-like shape in grain boundaries continuously. Moreover, the secondary phase particles are generally broken in the process of deformation. The dispersed secondary phase particles in matrix impede the dislocations motion during the deformation processing, leading to the dislocation pile-up and activation of the DRX [26]. In Mg−1.5Zn−0.6Zr−(0−4)Er alloys [27], the higher degree of DRX might be due to the high volume fraction of the secondary phase via particle-stimulated nucleation (PSN).

In the present work, although the volume fraction of the *I*-phase and the *W*-phase in the Mg−6Zn−1Er alloy (Alloy A) and Mg−2Zn−2Er alloy (Alloy B) was about the same, respectively, the mechanical properties of the two kinds of alloys were obviously different, which was amazing. The Mg−6Zn−1Er alloy (Alloy A) containing the *I*-phase consisted of uniaxial grains and broken micro-meter scale *I*-phase, as shown in Figs. 3(a) and (b). At the same time, the DRX via PSN introduced by the *I*-phase was activated. The DRX via PSN introduced by the *I*-phase contributed to the nucleation of new grains with a high orientation mismatch to the parent grains, resulting in random texture [28,29]. It is considered as the conventional DRX mechanism, i.e., discontinuous DRX mechanism (DDRX) which tends to form well-developed equiaxed recrystallized grains. However, the Mg−2Zn−2Er alloy (Alloy B) containing the *W*-phase consisted of finer grains, unDRXed deformed grains and broken micro-meter scale *W*-phase particles, as shown in Figs. 3(c) and (d). Besides, the unrecrystallized regions have serrated boundaries in the as-extruded Mg−2Zn−2Er alloy, which was the characteristic of the continuous DRX (CDRX) reported by TAHREEN et al [30]. The CDRX is essentially a one-step process, and the new developing grains are nucleated evenly throughout the material and could hardly grow [31]. In addition, KIM et al [32] has investigated the texture development and its effect on mechanical properties of AZ61 alloy, and the change of the strength was thought to be dependent on both the grain size and the texture. According to the Hall−Petch relationship, the grain refinement would lead to a high yield stress. Meanwhile, the softening texture was strongly attributed to the increase of Schmid factors of various slip systems, which made the yield stress decrease during tensile test.

Therefore, the as-extruded Mg−Zn−Er alloys containing *I*-phase showed a completely DRX microstructure with a grain size of ~9.7 μm while the grain size of the Mg−Zn−Er alloys containing *W*-phase was ~5.0 μm. The maximum texture intensity of the alloy containing *I*-phase was relatively low, i.e. 7.8, but the maximum texture intensity of the alloy containing *W*-phase was ~13.1. The *I*-phase had a special better effect on modifying the texture via DDRX, which resulted in a higher elongation. However, the *W*-phase played an important role in refining grain sizes via CDRX as well as a higher maximum texture intensity, which led to a higher tensile strength, especially the yield strength. In conclusion, the DRX of the Mg−Zn−Er alloy was mainly ascribed to the kinds of the secondary phases when the volume fractions of the secondary phases were the same.

5 Conclusions

1) Both the *I*-phase and the *W*-phase were broken and distributed along the extrusion direction.

2) The *I*-phase via particle-stimulated nucleation (PSN) had a great effect on modification of texture due to the discontinuous dynamic recrystallization mechanism (DDRX), which tended to form well-developed equiaxed recrystallized grains. Meanwhile, the *W*-phase played an important role in refining the grain size via continuous dynamic recrystallization (CDRX), companied with higher maximum texture intensity.

3) The Mg−6Zn−1Er alloy showed a performance of a higher elongation of 20.4%. The Mg−2Zn−2Er alloy displayed a better tensile strength, and the value of the YS was about 247 MPa.

References

[1] SINGH A, SOMEKAWA H, MUKAI T. High temperature processing of Mg−Zn−Y alloys containing quasicrystal phase for high strength [J]. Materials Science and Engineering A, 2011, 528: 6647−6651.

[2] LUO Su-qin, TANG Ai-tao, PAN Fu-sheng, SONG Kai, WANG Wei-qing. Effect of mole ratio of Y to Zn on phase constituent of Mg−Zn−Zr−Y alloys [J]. Transactions of Nonferrous Metals Society of China, 2011, 21: 795−800.

[3] SINGH A, WATANABE M, KATO A, TSAI A P. Microstructure and strength of quasicrystal containing extruded Mg−Zn−Y alloys for elevated temperature application [J]. Materials Science and Engineering A, 2004, 385: 382−396.

[4] LI Jian-hui, DU Wen-bo, LI Shu-bo, WANG Zhao-hui. Icosahedral quasicrystalline phase in an as-cast Mg−Zn−Er alloy [J]. Rare Metals, 2009, 28: 297−301.

[5] YUAN Guang-yin, LIU Yong, DING Wen-jiang, LU Chen. Effects of extrusion on the microstructure and mechanical properties of Mg−Zn−Gd alloy reinforced with quasicrystalline particles [J]. Materials Science and Engineering A, 2008, 474: 348−354.

[6] WEI Guo-bing, PENG Xiao-dong, ZHANG Bao, HADADZADEH A, XU Tian-cai, XIE Wei-dong. Influence of *I*-phase and *W*-phase on microstructure and mechanical properties of Mg−8Li−3Zn alloy [J]. Transactions of Nonferrous Metals Society of China, 2015, 25: 713−720.

[7] XU D K, TANG W N, LIU L, XU Y B, HAN E H. Effect of Y concentration on the microstructure and mechanical properties of as-cast Mg−Zn−Y−Zr alloys [J]. Journal of Alloys and Compounds, 2007, 432: 129−134.

[8] YANG Wen-peng, GUO Xue-feng. High strength magnesium alloy with *α*-Mg and *W*-phase processed by hot extrusion [J]. Transactions of Nonferrous Metals Society of China, 2011, 21: 2358−2364.

[9] YANG Q, XIAO B L, MA Z Y, CHEN R S. Achieving high strain rate superplasticity in Mg−Zn−Y−Zr alloy produced by friction stir processing [J]. Scripta Materialia, 2011, 65: 335−338.

[10] XU D K, LIU L, XU Y B, HAN E H. The influence of element Y on the mechanical properties of the as-extruded Mg−Zn−Y−Zr alloys [J]. Journal of Alloys and Compounds, 2006, 426: 155−161.

[11] MA Q, LI B, WHITTINGTON W R, OPPEDAL A L, WANG P T, HORSTEMEYER M F. Texture evolution during dynamic

recrystallization in a magnesium alloy at 450 °C [J]. Acta Materialia, 2014, 67: 102−115.
[12] XU S W, ZHENG M Y, KAMADO S, WU K, WANG G J, LV X Y. Dynamic microstructural changes during hot extrusion and mechanical properties of a Mg−5.0Zn−0.9Y−0.16Zr (wt.%) alloy [J]. Materials Science and Engineering A, 2011, 528: 4055−4067.
[13] KIM W J, HONG S I, KIM Y S, MIN S H, JEONG H T, LEE J D. Texture development and its effect on mechanical properties of an AZ61 Mg alloy fabricated by equal channel angular pressing [J]. Acta Materialia, 2003, 51: 3293−3307.
[14] MISHRA R K, GUPTA A K, RAO P R, SACHDEV A K, KUMAR A M, LUO A A. Influence of cerium on the texture and ductility of magnesium extrusions [J]. Scripta Materialia, 2008, 59: 562−565.
[15] STANFORD N, ATWELL D, BARNETT M R. The effect of Gd on the recrystallisation, texture and deformation behaviour of magnesium-based alloys [J]. Acta Materialia, 2010, 58: 6773−6783.
[16] SADEGHI A, HOSEINI M, PEKGULERYUZ M. Effect of Sr addition on texture evolution of Mg−3Al−1Zn (AZ31) alloy during extrusion [J]. Materials Science and Engineering A, 2011, 528: 3096−3104.
[17] WANG Yan-nan, XIN Yun-chang, YU Hui-hui, LV Liang-chen, LIU Qing. Formation and microstructure of shear bands during hot rolling of a Mg−6Zn−0.5Zr alloy plate with a basal texture [J]. Journal of Alloys and Compounds, 2015, 644: 147−154.
[18] XU S W, CHEN R S, KAMADO S, HONMA T, HAN E H. Twins, shear bands and recrystallization of a Mg−2.0%Zn−0.8%Gd alloy during rolling [J]. Scripta Materialia, 2011, 64: 141−144.
[19] SITDIKOV O, KAIBYSHEV R. Dynamic recrystallization in pure magnesium [J]. Materials Transactions, 2001, 42: 1928−1937.
[20] LIU Ke, SUN Cui-cui, WANG Zhao-hui, LI Shu-bo, WANG Qing-feng, DU Wen-bo. Microstructure, texture and mechanical properties of Mg−Zn−Er alloys containing *I*-phase and *W*-phase simultaneously [J]. Journal of Alloys and Compounds, 2016, 665: 76−85.
[21] HUANG Hua, TANG Zi-bo, TIAN Yuan, JIA Gao-zhi, NIU Jia-lin, ZHANG Hua, PEI Jia, YUAN Guang-yin, DING Wen-jiang. Effects of cyclic extrusion and compression parameters on microstructure and mechanical properties of Mg−1.50Zn−0.25Gd alloy [J]. Materials and Design, 2015, 86: 788−796.
[22] LI Han, DU Wen-bo, LI Shu-bo, WANG Zhao-hui. Effect of Zn/Er weight ratio on phase formation and mechanical properties of as-cast Mg−Zn−Er alloys [J]. Materials and Design, 2012, 35: 259−265.
[23] LIU Ke, WANG Qing-feng, DU Wen-bo, LI Shu-bo, WANG Zhao-hui. Failure mechanism of as-cast Mg−6Zn−2Er alloy during tensile test at room temperature [J]. Transactions of Nonferrous Metals Society of China, 2013, 23: 3193−3199.
[24] SINGH A, WATANABE M, KATIO A,TSAI A P. Twinning and the orientation of icosahedral phase with the magnesium matrix [J]. Acta Materialia, 2005, 53: 4733−4742.
[25] HUANG Hua, TIAN Yuan, YUAN Guang-yin, CHEN Chun-lin, WANG Zhong-chang, DING Wen-jiang, INOUE A. Dislocations in icosahedral quasicrystalline phase embedded in hot-deformed Mg alloys [J]. Journal of Alloys and Compounds, 2016, 658: 483−487.
[26] DOHERTY R D, HUGHES D A, HUMPHREYS F J, JONAS J J, JENSEN D J, KASSNER M E, KING W E, McNELLEY T R, McQUEEN H J, ROLLETT A D. Current issues in Recrystallization: A review [J]. Materials Science and Engineering A, 1997, 238: 219−274.
[27] ZHANG Jing, LI Wei-guo, GUO Zheng-xiao. Static recrystallization and grain growth during annealing of an extruded Mg−Zn−Zr−Er magnesium alloy [J]. Journal of Magnesium and Alloys, 2013, 1: 31−38.
[28] LEE J Y, LIM H K, KIM D H, KIM W T, KIM D H. Effect of icosahedral phase particles on the texture evolution in Mg−Zn−Y alloys [J]. Materials Science and Engineering A, 2008, 491: 349−355.
[29] LIU Yong, YUANG Guang-yin, CHEN Lu, DING Wen-jiang, JIANG Jiang-zhong. The role of nanoquasicrystals on the ductility enhancement of as-extruded Mg−Zn−Gd alloy at elevated temperature [J]. Journal of Materials Science, 2008, 43: 5527−5533.
[30] TAHREENA N, ZHANG D F, PAN F S, JIANG X Q, LI D Y, CHEN D L. Hot deformation and processing map of an as-extruded Mg−Zn−Mn−Y alloy containing *I* and *W* phases [J]. Materials and Design, 2015, 87: 245−255.
[31] YANG X Y, MIURA H, SAKAI T. Dynamic evolution of new grains in magnesium alloy AZ31 during hot deformation [J]. Materials Transactions, 2003, 44: 197−203.
[32] KIM W J, HONG S I, KIM Y S, MIN S H, JEONG H T, LEE J D. Texture development and its effect on mechanical properties of an AZ61 Mg alloy fabricated by equal channel angular pressing [J]. Acta Materialia, 2003, 51: 3293−3307.

第二相对挤压态 Mg−Zn−Er 合金织构及力学性能的影响

刘 轲[1]，刘金学[1]，李淑波[1]，王朝辉[1]，杜文博[1]，王庆峰[2]

1. 北京工业大学 材料科学与工程学院，北京 100124；
2. 华电电力科学研究院，北京 100124

摘 要：研究不同的第二相对 Mg−Zn−Er 合金的织构及力学性能的影响。结果表明，准晶 *I* 相通过引起不连续动态再结晶机制(DDRX)而形成大量的等轴晶，进而弱化织构；而 *W* 相则通过连续动态再结晶机制(CDRX)对细化晶粒起到很重要的作用，且具有较高的织构强度。因此，含有 *I* 相的 Mg−6Zn−1Er 合金具有较高伸长率，为 20.4%；而含有 *W* 相的 Mg−2Zn−2Er 合金则表现了更好的强度，其屈服强度(YS)约为 247 MPa。

关键词：Mg−Zn−Er 合金；动态再结晶；织构；拉伸性能

(Edited by Bing YANG)